



SIMULATING REFLECTIVITY PROPERTY FOR PROPAGATING WAVE INSIDE ONE-DIMENSIONAL PHOTONIC CRYSTAL WITH DIFFERENT MATERIAL SYSTEMS

Sourangsu Banerji¹, Arpan Deyasi²

¹Cognizant Technology Solutions, ²RCC Institute of Information Technology West Bengal, INDIA-700015
sourangsu.banerji@gmail.com

Received 8-02-2015, online 1-03-2015

ABSTRACT

In this paper, reflective coefficient due to electromagnetic wave propagation in forward and backward directions inside one-dimensional photonic crystal is theoretically computed using coupled mode theory. Coupling coefficient and material composition are varied to study the possible change in wave propagation in the bounded medium. Grating length is tuned for near accurate computation of the stratified periodic structure. The periodic dielectric array is essentially a Bragg grating where increase in grating length enhances the reflection of electromagnetic wave, and strong coupling provides larger bandgap spectral width. For simulation purpose, GaN/Al_xGa_{1-x}N material composition is considered as unit block of the periodic organization, and refractive index of Al_xGa_{1-x}N is taken as function of bandgap and operating wavelength following Adachi's model. Results are compared with that obtained for SiO₂/air material system for identical structural parameters and other propagating conditions. Simulation proves the dominance of usability of semiconductor heterostructure-based photonic crystal for optical communication in comparison to the conventional system.

Keywords: One-Dimensional Photonic Crystal, Forward and Backward Waves, Bragg Wavelength, Reflectivity, Strong and Weak Coupling

I. INTRODUCTION

Photonic crystal is a periodic arrangement of dielectric materials [1] where localization of electromagnetic wave propagating inside the structure is controlled by controlled tuning the structural parameters. This is possible due to the formation of photonic bandgap, a property which is extensively used in photonic integrated circuits [2], optical transmitter [3], optical receiver [4], photonic crystal fiber [5], quantum information processing [6] etc. This novel microstructure has already replaced conventional optical fiber for efficient communication. Various types of confinements has already been

considered by theoretical researchers for analysis of photonic crystal, but it is suggested that only 1D and 2D structures are efficient enough to realize experimentally and for implementation purpose in different optoelectronic integrated circuits. Among them, 1D structure is very convenient to study because of ease of mathematical modelling. Propagating wave analysis in 1D structure is useful for designing four-wave mixing analysis in nonlinear photonic crystal [7]. Suitable dielectric materials are used to characterize modal dispersion in 1D crystal [8]. Incorporation of semiconductor nanostructure makes it more interesting when filter characteristics is considered [9]

including the effect of polarization of incident light. The present paper deals with simulating characteristics of forward and backward electromagnetic waves as a function of grating length in one-dimensional photonic crystal when Bragg wavelength is set at 1550 nm for both $\text{Al}_x\text{Ga}_{1-x}\text{N}/\text{GaN}$ and SiO_2/Air composition. Coupled mode theory has been used to solve the problem using Bragg condition. Refractive indices of the materials are considered as function of material composition (x) specifically in the case $\text{Al}_x\text{Ga}_{1-x}\text{N}/\text{GaN}$, bandgap and operating wavelength. Reflectivity is computed from the knowledge of wave propagation for different coupling conditions. The spectral width of the structure i.e., photonic bandgap is measured from the reflection coefficient analysis. Use of $\text{AlGaIn}/\text{GaIn}$ material composition is taken up because as shown in [10], the predominant effect of carrier localization in undoped AlGaIn alloys enhances with the increase in Al contents, being related to the insulating nature of AlGaIn of high Al contents. High Al-content in AlGaIn layer also increases the overall figure of merit of the $\text{AlGaIn}/\text{GaIn}$ due to the combined advantages of enhanced band offset, lattice mismatch induced piezoelectric effect. The advantages of GaN can be summarized as ruggedness, power handling and low loss [11, 12].

The organization of the paper is as follows; in section 2 working mathematical model is discussed based on coupled mode theory. In section 3, we obtain the simulation results for both $\text{Al}_x\text{Ga}_{1-x}\text{N}/\text{GaN}$ and SiO_2/Air material composition and compared for identical structural and coupling parameters. Lastly, summarization is made based on obtained results.

II. MATHEMATICAL MODELING

Coupled mode theory is being applied to counter-propagating waves in a single mode one dimensional periodic structure i.e. Bragg grating with a periodic corrugation as shown in Fig. 1.

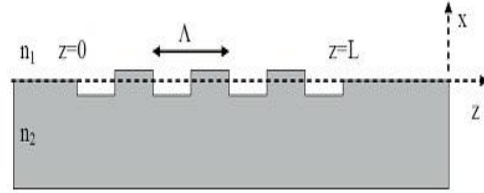


Figure 1: Periodic corrugation in one of the core-cladding interfaces. The grating is single mode, and we make the assumption that the only significant coupling is between counter propagating guided modes

The corrugation is scalar and we don't expect coupling between TE and TM modes, so in the following treatment we'll consider TE modes. We start by describing the field in the corrugated structure as a sum of the forward and backward propagating modes

$$E_y = A(z)u(x)\exp[j(\omega.t - \beta.z)] + B(z)u(x)\exp[j(\omega.t - \beta.z)] \quad (1)$$

where A and B are the amplitudes of the forward and backward propagating waves, and $u(x)$ is the mode profile.

The perturbation in the corrugated region is

$$\vec{P}_{pert} = \Delta n(x, z)^2 \epsilon_0 \vec{E} \quad (2)$$

We now substitute the expression for the field into this expression to get

$$P_{pert} = \frac{1}{2} \Delta n(x)^2 \epsilon_0 \times \left\{ A(z)u(x)\exp[j(\omega.t - \beta.z)] + B(z)u(x)\exp[j(\omega.t - \beta.z)] \right\} \quad (3)$$

$$P_{pert} = \frac{1}{2} \Delta n(x)^2 \epsilon_0 e^{j\omega.t} e^{-j\beta.z} \times \left\{ A + B e^{j2\beta.z} \right\} u(x). \quad (4)$$

Recalling the fundamental coupled mode equation

$$-\frac{dA_i^+}{dz} \cdot \exp[j(\omega t - \beta \cdot z)] + \frac{dA_i^-}{dz} \cdot \exp[j(\omega t + \beta \cdot z)] + c.c \quad (5)$$

$$= -\frac{j}{2\omega} \frac{\partial^2}{\partial t^2} \int_{-\infty}^{\infty} P_{pert}(x, z, t) \cdot u_i(x) dx$$

which simplifies to

$$-\frac{dA}{dz} + \frac{dB}{dz} e^{j2\beta \cdot z} = \frac{-j\omega \cdot \epsilon_0}{4} \{A + B e^{j2\beta \cdot z}\} \int_{-\infty}^{\infty} \Delta n^2 u^2(x) dx. \quad (6)$$

We will now assume that the corrugation has a square-wave shape as indicated in Fig. 1. The general conclusions are not dependent on the exact shape, so the following treatment, with appropriate adjustments, is valid also for non-square corrugations. The square-wave corrugations can be expressed as a series in the following form

$$\Delta n^2(x, z) = \Delta n^2 \sum_m C_m e^{j \cdot \frac{2m\pi \cdot z}{\Lambda}} \quad (7)$$

$$C_m = \begin{cases} -\frac{j}{m\pi} & m = \text{odd} \\ 0 & m = \text{even} \end{cases}. \quad (8)$$

By comparing this expression to the above coupled mode equations, we realize that only modes that are close to phase matched will experience significant coupling. In other words, we need only keep terms of the same periodicity. In a range of wave vectors, the equations can be simplified to

$$\frac{dA}{dz} = \frac{j\omega \cdot \epsilon_0}{4} B e^{j2\beta \cdot z} C_m e^{-j \cdot \frac{2m\pi \cdot z}{\Lambda}} \times \int_{-\infty}^{\infty} \Delta n^2 u^2(x) dx \quad (9)$$

$$\frac{dB}{dz} = \frac{j\omega \cdot \epsilon_0}{4} A e^{-j2\beta \cdot z} C_m e^{j \cdot \frac{2m\pi \cdot z}{\Lambda}} \times \int_{-\infty}^{\infty} \Delta n^2 u^2(x) dx \quad (10)$$

$$\frac{dA}{dz} = K^* B e^{j2\Delta\beta \cdot z} \quad (11)$$

$$\frac{dB}{dz} = K A e^{-j2\Delta\beta \cdot z} \quad (12)$$

$$K = C_m e^{j \cdot \frac{2m\pi \cdot z}{\Lambda}} \int_{-\infty}^{\infty} \Delta n^2 u^2(x) dx \quad (13)$$

where

$$\Delta\beta = \beta - \frac{m\pi}{\Lambda}. \quad (14)$$

Let us check energy conservation in the systems of equations we have found for modes in a Bragg grating i.e. one-dimensional periodic dielectric array. We start by deriving expression for the energies in the forward and backward propagating waves. Based on eqn. 1 we can write

$$\frac{d}{dz} |A|^2 = A \cdot \frac{dA^*}{dx} + A^* \cdot \frac{dA}{dx} \quad (15)$$

$$= A \cdot B^* \cdot K e^{-j2\Delta\beta \cdot z} + A^* \cdot B \cdot K^* e^{j2\Delta\beta \cdot z}$$

$$\frac{d}{dz} |B|^2 = B \cdot \frac{dB^*}{dx} + B^* \cdot \frac{dB}{dx} \quad (16)$$

$$= B \cdot A^* \cdot K^* e^{j2\Delta\beta \cdot z} + B^* \cdot A \cdot K e^{-j2\Delta\beta \cdot z}.$$

The difference between the rates of change in the forward-propagating and backward-propagating energy is then

$$\begin{aligned} \frac{d}{dz} |A|^2 - \frac{d}{dz} |B|^2 = & A \cdot B^* \cdot K e^{-j2\Delta\beta \cdot z} + A^* \cdot B \cdot K^* e^{j2\Delta\beta \cdot z} \\ & - B^* \cdot A \cdot K e^{-j2\Delta\beta \cdot z} - B \cdot A^* \cdot K^* e^{j2\Delta\beta \cdot z}. \end{aligned} \quad (17)$$

Eq. (17) becomes zero due to the equilibrium, so that

$$\frac{d}{dz} |A|^2 - \frac{d}{dz} |B|^2 = 0. \quad (18)$$

We see that the rate of change in forward-propagating energy is exactly balanced by the rate of change in backward-propagating energy, which is the correct result for loss-less, counter-propagating waves.

The set of equations describing the modes of the Bragg grating (Eqns. 9-13) can now be solved. Assuming that the forward propagating mode has an

amplitude A_0 at $z = 0$, and that the backward propagating wave is zero at $z = L$, we find

$$A = A_0 e^{j\Delta\beta \cdot z} \times \frac{-\Delta\beta \sinh[S(z-L)] + jS \cosh[S(z-L)]}{-\Delta\beta \sinh[SL] + jS \cosh[SL]} \quad (18)$$

$$A = A_0 e^{j\Delta\beta \cdot z} \times \left[\frac{-\Delta\beta \sinh[S(z-L)]}{-\Delta\beta \sinh[SL] + jS \cosh[SL]} + \frac{jS \cosh[S(z-L)]}{-\Delta\beta \sinh[SL] + jS \cosh[SL]} \right] \quad (19)$$

$$B = A_0 \cdot jK \cdot e^{-j\Delta\beta \cdot z} \times \frac{\sinh[S(z-L)]}{-\Delta\beta \sinh[SL] + jS \cosh[SL]} \quad (20)$$

where

$$S = \sqrt{K^2 - \Delta\beta^2} \quad (21)$$

When $\Delta\beta \rightarrow 0$, this simplifies to

$$A = A_0 \frac{\cosh[K(z-L)]}{\cosh[KL]} \quad (22)$$

$$B = A_0 \cdot \frac{\sinh[K(z-L)]}{\cosh[KL]} \quad (23)$$

The expressions we have found for the field amplitudes in the periodically corrugated waveguide allow us to calculate the reflection and transmission spectra of the Bragg grating. For example, the field reflection is simply the ratio of the forward propagating and backward propagating wave at the input to the Bragg grating:

$$r = \frac{B(0)}{A(0)} = \frac{A_0 \cdot jK \frac{\sinh[SL]}{-\Delta\beta \sinh[SL] + jS \cosh[SL]}}{A_0 \cdot \frac{-\Delta\beta \sinh[SL] + jS \cosh[SL]}{-\Delta\beta \sinh[SL] + jS \cosh[SL]}} \quad (24)$$

The ratio can be simplified in the following form

$$r = jK \frac{\sinh[SL]}{-\Delta\beta \sinh[SL] + jS \cosh[SL]} \quad (25)$$

III. RESULTS AND DISCUSSION

Using Eq. (18) and Eq. (20), forward and backward electromagnetic waves are calculated as a function of grating length for $\text{Al}_x\text{Ga}_{1-x}\text{N}/\text{GaN}$ and SiO_2/Air material composition under the different conditions of coupling. The input wavelength is kept equal to the Bragg wavelength as it can be proved that magnitude of wave is the maximum when input wavelength matches with Bragg wavelength, which is the resonance condition. Fig. 2a shows the profile for forward waves for both $\text{Al}_x\text{Ga}_{1-x}\text{N}/\text{GaN}$ and SiO_2/Air composition under the action of weak coupling ($\kappa = 0.01$) whereas Fig.2b is plotted for forward waves under strong coupling ($\kappa = 0.05$) conditions waves.

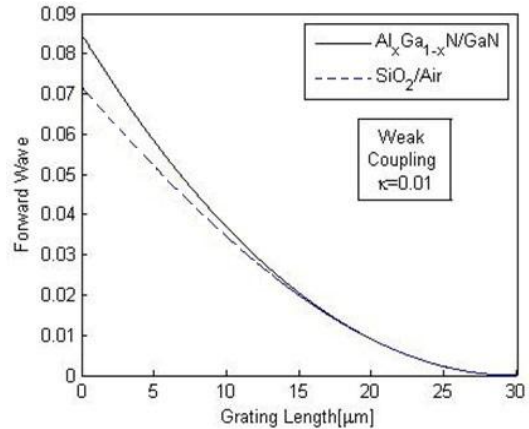


Figure 2a: Forward wave profile with increasing grating length for $\text{Al}_x\text{Ga}_{1-x}\text{N}/\text{GaN}$ and SiO_2/Air material composition under weak coupling conditions

From Fig.2, it is seen that the forward wave characteristics for both the compositions differ in magnitude for smaller grating length (say only up to 10 μm) under weak coupling conditions. However as the grating length increases

magnitude in both the cases is so close to each other that it is quite indistinguishable to tell them apart. The main thing to note is that $\text{Al}_x\text{Ga}_{1-x}\text{N}/\text{GaN}$ composition gives us a better response for forward wave characteristics for weak coupling in the structure.

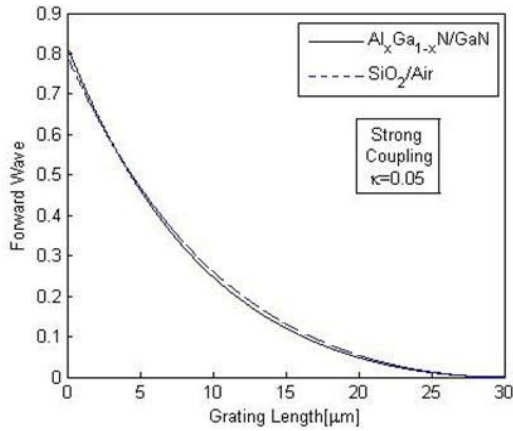


Figure 2b: Forward wave profile with increasing grating length for $\text{Al}_x\text{Ga}_{1-x}\text{N}/\text{GaN}$ and SiO_2/Air material composition under strong coupling conditions

Fig.2b similarly depicts the forward wave profile for $\text{Al}_x\text{Ga}_{1-x}\text{N}/\text{GaN}$ and SiO_2/Air material composition with varying grating length under strong coupling action ($\kappa = 0.05$). No anomaly is seen here as compared to the previous case of weak coupling. Rather, in the case of strong coupling the magnitude curves for both the compositions are nearly the same except in some minor places which helps us to distinguish between the two curves.

Fig. 3 plots the backward wave profile with the increase in the length of the grating under similar conditions of coupling i.e. both weak and strong for both $\text{Al}_x\text{Ga}_{1-x}\text{N}/\text{GaN}$ and SiO_2/Air material composition. In Fig. 3a, the backward wave magnitude for the $\text{Al}_x\text{Ga}_{1-x}\text{N}/\text{GaN}$ composition is less than the SiO_2/Air case and the difference between the respective curves increases in magnitude with the increase in grating

length. This observation is very important because it highlights the fact that with increasing grating length the decrease in the backward wave magnitude is of some order more in $\text{Al}_x\text{Ga}_{1-x}\text{N}/\text{GaN}$ compared to SiO_2/Air under weak coupling conditions.

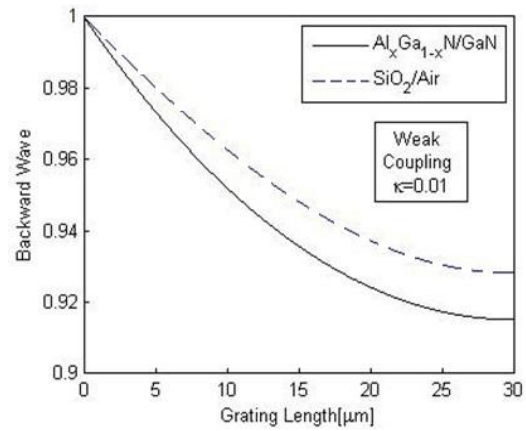


Figure 3a: Backward wave profile with increasing grating length for $\text{Al}_x\text{Ga}_{1-x}\text{N}/\text{GaN}$ and SiO_2/Air material composition under weak coupling conditions

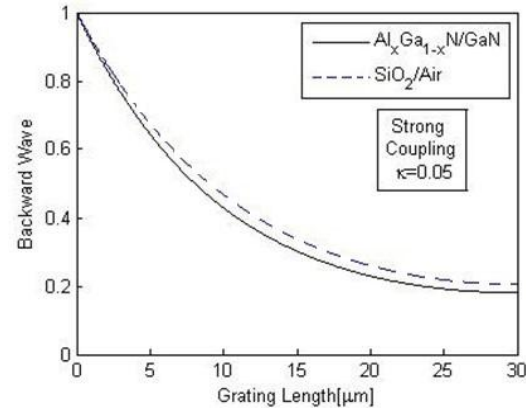


Figure 3b: Backward wave profile with increasing grating length for $\text{Al}_x\text{Ga}_{1-x}\text{N}/\text{GaN}$ and SiO_2/Air material composition under strong coupling conditions

Similarly, in case of strong coupling here still no anomalous behavior is seen. Rather the behavior is pretty predictable. Here also the magnitude of the backward wave of the $\text{Al}_x\text{Ga}_{1-x}\text{N}/\text{GaN}$ based composition is much less than the SiO_2/Air composition. But the difference

in magnitude between both the curves is not much wide as seen in the previous case. There is a gradual decrease in the strength of the backward wave for both the cases under the action of strong coupling.

One remarkable observation which we get from both Fig 2a and 2b as well as Fig 3a and 3b is that when the coupling between the forward and the backward wave is weak ($\kappa=0.01$), with the increase in grating length, more of the waves move forward as compared to moving backward which is very predominantly seen in case of the $\text{Al}_x\text{Ga}_{1-x}\text{N}/\text{GaN}$ based composition. The SiO_2/Air material composition does not show such a distinguishable behavior. For the strong coupling case ($\kappa=0.05$), the behavior is not that sharp for both the material composition. Overall we can claim that under both conditions of coupling especially for the backward wave, the value is lowest for resonance condition, which eventually satisfies the energy conservation principle. The difference in magnitude increases with higher value of grating length.

IV. Conclusion

In this paper, we have rigorously studied the effect of the coupling and reflectivity on the propagation of electromagnetic magnetic waves in one dimensional periodic structure known as photonic crystals by varying the length of the grating and also fabrication them with different material composition namely, $\text{Al}_x\text{Ga}_{1-x}\text{N}/\text{GaN}$ and SiO_2/Air . The corresponding results and plots obtained from $\text{Al}_x\text{Ga}_{1-x}\text{N}/\text{GaN}$ composition were matched with that of SiO_2/Air and analyzed. Observation revealed that $\text{Al}_x\text{Ga}_{1-x}\text{N}/\text{GaN}$ composition

outperformed SiO_2/Air in every aspect that was studied in this paper. The general characteristics of wave propagation revealed that in SiO_2/Air composition the magnitude of forward and backward wave propagation was correspondingly less as well as more compared to its counterpart $\text{Al}_x\text{Ga}_{1-x}\text{N}/\text{GaN}$. Finally, in conclusion we can say from the reflectivity profiles that designing bandpass filters at optical communication spectra using one-dimensional photonic crystals structures will prove beneficial if fabrication is done with semiconductor heterostructures like $\text{Al}_x\text{Ga}_{1-x}\text{N}/\text{GaN}$ over conventional ones like SiO_2/Air .

References

- [1] E. Yablonovitch, "Inhibited Spontaneous Emission in Solid-State Physics and Electronics", *Physical Review Letters*, **58**, 2059-2061 (1987).
- [2] K. Bayat, G. Z. Rafi, G. S. A. Shaker, N. Ranjkesh, S. K. Chaudhuri and S. Safavi-Naeini, "Photonic-Crystal based Polarization Converter for Terahertz Integrated Circuit", *IEEE Transactions on Microwave Theory and Techniques*, **58**, 1976-1984 (2010).
- [3] P. Szczepanski, "Semiclassical Theory of Multimode Operation of a Distributed Feedback Laser", *IEEE Journal of Quantum Electronics*, **24**, 1248-1257 (1988).
- [4] I. S. Fogel, J. M. Bendickson, M. D. Tocci, M. J. Bloemer, M. Scalora, C. M. Bowden and J. P. Dowling, *Pure and Applied Optics*, "Spontaneous Emission and Nonlinear Effects in Photonic Bandgap Materials", **7**, 393-408 (1998).
- [5] P. S. J. Russell, "Photonic-Crystal Fibers", *Journal of Lightwave Technology*, **24**, 4729-4749 (2006).
- [6] H. Azuma, "Quantum Computation with Kerr-Nonlinear Photonic Crystals", *Journal of Physics D: Applied Physics*, **41**, 025102 (2008).

[7] M Boozarjmehr, "FWM in one-Dimensional Nonlinear Photonic Crystal and Theoretical Investigation of Parametric Down Conversion Efficiency (Steady State Analysis)", Proceedings of the International Multiconference of Engineers and Computer Scientists, March, **11**, Hong-Kong (2009).

[8] S Prasad, V Singh and A K Singh, "To Control the Propagation Characteristic of One-Dimensional Plasma Photonic Crystal using Exponentially Graded Dielectric Material", Progress in Electromagnetic Research M, **22**, 123-126 (2012).

[9] A. Maity, B. Chottopadhyay, U. Banerjee, A. Deyasi, "Novel Band-Pass Filter Design using Photonic Multiple Quantum Well Structure with p-polarized Incident Wave at 1550 μm ", Journal of Electron Devices, **17**, 1400-1405 (2013).

[10] M. D. Hodge, R. Vetury and J. B. Shealy, "Fundamental failure mechanisms limiting maximum voltage operation in AlGaIn/GaN HEMTs", IEEE International Reliability Physics Symposium, Anaheim (2012) pp. 1-6.

[11] M. Hadis, "Handbook of Nitride Semiconductors and Devices", GaN-based Optical and Electronic Devices, **3**, Wiley (2009).

[12] P. C. Hoang, "Applications of Photonic Crystals in Communications Engineering and Optical Imaging", PhD Thesis, D-67663 Kaiserslautern,. Geburtsort: Hanoi Vietnam (2009).